CHEMISTRY & SUSTAINABILITY
CHEMSUSCHEM
ENERGY & MATERIALS

Accepted Article

Title: Heterogeneous rhenium oxide modified iridium catalyzed one-pot conversion of lignin into naphthenes

Authors: Changzhi Li, Bo Zhang, Xinxin Li, Xiaoli Pan, Jianwei Ji, Yujing Ren, Hua Wang, Na Ji, and Qiying Liu

To be cited as: *ChemSusChem* 10.1002/cssc.201903286

Link to VoR: http://dx.doi.org/10.1002/cssc.201903286

A Journal of ChemPubSoc Europe

WILEY-VCH www.chemsuschem.org

Heterogeneous rhenium oxide modified iridium catalyzed one-port conversion of lignin into naphthenes

Xinxin Li,[a][b]† Bo Zhang,[a]† Xiaoli Pan,[a] Jianwei Ji,[c] Yujing Ren,[a] Hua Wang,[a] Na Ji,*[b] Qiying Liu,[d][e] Changzhi Li*[a][e]

Abstract: Direct transformation of lignin into fuels and chemicals remains huge challenge due to the stubborn and complicated lignin structure. Here rhenium oxide modified iridium supported by SiO_2 (Ir-ReO_x/SiO_2) was employed for one-pot conversion of various lignin model compounds and lignin feedstocks into naphthenes. Up to 100% yield of cyclohexane from model compounds and 44.3% yield of naphthenes from lignin feedstocks were achieved. 2D HSQC NMR analysis before and after reaction confirmed the clear activity of Ir-ReO_x/SiO_2 in cleavage of the C-O bonds and hydrodeoxygenation of the depolymerized products. H_2-temperature-programed reduction (H_2-TPR), temperature-programmed desorption of NH_3 (NH_3-TPD), IR spectroscopy of pyridine adsorption (pyridine-IR), X-ray photoelectron spectroscopy (XPS) and X-ray absorption fine structure (XAFS) characterization, as well as control experiments revealed that a synergistic effect between Ir and ReO_x in Ir-ReO_x/SiO_2 played a crucial role for the high performance; of which, ReO_x was mainly responsible for the cleavage of C-O bonds whilst Ir was in charge of HDO reaction and saturation of the benzene rings. This methodology opens an energy-efficient route for directly converting lignin into valuable naphthenes.

Introduction

With reducing the consumption of petroleum and concerning on the growth of environment issues, the conversion of renewable biomass to liquid fuels has attracted increasing attention.[1] Lignocellulose, the most abundant form of biomass, is a renewable energy resource for the production of transportation fuels.[2] As a major component in lignocellulose, lignin is regarded as a waste product in pulp industry, and is often treated to supply heat through burning or discarded.[3] From the chemical structure of lignin, one can expect that it is a unique candidate for the production of fuels and a wide variety of aromatic chemicals.[4] However, the inactive property and the complexity of lignin make it notorious resistant to chemical transformation, and effective dissembling of lignin represents a huge challenge. So far, great efforts have been achieved to address this challenge. One of the most important and popular depolymerization method to produce fuels is catalytic hydrodeoxygenation (HDO). For example, numerous research groups have employed lignin monomers (phenols, guaiacols, syringols and their derivatives) to assess the potential for the transformation of lignin to fuels.[5] Further, phenolic bio-oil, produced by fast pyrolysis or catalytic depolymerization of lignin, is tested for the production of naphthenes via HDO reaction over different heterogeneous catalysts.[6] From the perspectives of application, the development of advanced catalytic approaches for feasible one-pot conversion of lignin into naphthenes would be benefit for cost-effective utilization of biomass and is highly desirable, as indicated by pioneer works of Rinaldi,[7] Zhao,[8] and Wang[9] groups.

Rhenium (Re) possesses low electronegative and has wide range of oxidation states, hence can be used as a versatile catalyst in various reactions including biomass conversion.[10] It is reported that homogeneous methyltrioxorhenium (MTO)[11] and supported ReO_x catalysts[12][13] have the ability to remove two adjacent hydroxy groups of polyols to obtain alkenes via deoxydehydration (DODH) reaction. In the area of lignin conversion, Crestini[14], Kühn[15] and our own[16] groups show that rhenium-based catalysts such as MTO, Re_2O_7 and particularly ReO_x/AC[16c,16d] can effective cleavage of lignin C-O bonds, however, the products are the mixture of aromatic monomers and oligomers with the latter ones as the major component when meeting realistic lignin, making the subsequent utilization challenging and increasing difficulty in energy-intensive separation/purification process.

In comparison with the monometallic catalyst, the use of bimetallic catalysts is a promising strategy to modify the catalyst property, which would increase both the activity and stability of the catalyst, and tailor the selectivity to a particular product. Noting that platinum-group metals (PGMs) such as Pd, Pt and Ir, including non-noble metal Ni bear intrinsic properties in hydrogen activation, it offers the possibility to modify the surface properties of rhenium-based catalysts and improve the capability in hydrogen-involved reactions. Herein, we prepare a series of bimetallic catalysts composed of rhenium oxide and transition metals for the directly catalyzing both lignin model compounds and lignins into naphthenes. A clear synergistic effect is observed

---

[a] X. Li, Associate Prof. B. Zhang, X. Pan, Y. Ren, H. Wang, Prof. C. Li,
CAS Key Laboratory of Science and Technology on Applied Catalysis, Dalian Institute of Chemical Physics, Chinese Academy of Sciences, Dalian 116023, China
E-mail: licz@dicp.ac.cn, jina@tju.edu.cn
[b] X. Li, Associate Prof. N. Ji
School of Environmental Science and Engineering, Key Laboratory of Biomass-Derived Gas and Oil for Chinese Petrochemical Industry, Tianjin University, Tianjin 300350, China.
[c] Dr. J. Ji
Shaanxi Key Laboratory of Catalysis, School of Chemistry and Environment Science, Shaanxi Sci-tech University, 1 Dongyihuan Road, Hanzhong, 723001, China
[d] Prof. Q. Liu
Guangzhou Institute of Energy Conversion, Chinese Academy of Sciences, Guangzhou 510640, China
[e] Prof. Q. Liu, Prof. C. Li,
Dalian National Laboratory for Clean Energy, 457 Zhongshan Road, Dalian, 116023, China

[†] These authors contributed equally to this work.
Supporting information for this article is given via a link at the end of the document.((Please delete this text if not appropriate))

and Ir-ReO$_x$/SiO$_2$ exhibits extraordinarily high catalytic activity, representing one-pot conversion of realistic lignin into naphthenes.

Results and Discussion

Screening of the catalyst for the hydrodeoxygenation of phenethoxybenzene

A series of heterogeneous rhenium oxide modified metal catalysts composed of different metal sites and supports are prepared by wetness impregnation of metal precursors followed by a thermal treatment under air. Because lignin structure is notoriously complicated[3a], in our initial study, lignin model compound phenethoxybenzene is employed to assess the activity of various catalysts.

As shown in Figure 1, sole support SiO$_2$ and monometallic catalysts Ir/SiO$_2$ and ReO$_x$/SiO$_2$ exhibited very poor activity in the conversion of phenethoxybenzene, providing yields of cyclohexane and ethyl-cyclohexane less than 5%. In comparison, the physical mixture of Ir/SiO$_2$ and ReO$_x$/SiO$_2$ lead to an obvious increase in catalytic activity, yielding cyclohexane and ethyl-cyclohexane at 15% and 1%, respectively, probably due that the Re species mixed with noble metal Ir also can work as catalytic center for hydrogenation and C-O bonds cleavage.[10c] Interestingly, the bimetallic Ir-ReO$_x$/SiO$_2$ significantly speeded up the transformation process and displayed 97% yield of cyclohexane, 11% yield of methyl-cyclohexane, and 85% yield of ethyl-cyclohexane with almost complete conversion, highlighting the gratifying synergistic effects between Ir and ReO$_x$.

The conversion of various transition metals of Ir, Pd, Pt and Ni modified by rhenium oxide were compared. Figure 1 shows that Ni-ReO$_x$/SiO$_2$ gave the lowest conversion and yields of the products, and Pd-ReO$_x$/SiO$_2$, Pt-ReO$_x$/SiO$_2$ provided higher activity. For the latter two catalysts, incomplete hydrogenation products such as ethylbenzene (85% and 12% yields over Pd-ReO$_x$/SiO$_2$ and Pt-ReO$_x$/SiO$_2$, respectively) and cyclohexanol (7% and 8% yields over Pd-ReO$_x$/SiO$_2$ and Pt-ReO$_x$/SiO$_2$, respectively) were formed as the major by-products. Hence, Ir acting as the second metal exhibited better performance of HDO than the other three transition metals.

Bimetallic catalysts composed of Ir and various metallic oxides such as WO$_x$, MoO$_x$, VO$_x$, and MnO$_x$ were then prepared for the conversion of phenethoxybenzene. The results in Figure 1 shows that both the conversion (<50%) and the yield of naphthenes (<38%) dramatically decreased in all cases, as compared to the performance of Ir-ReO$_x$/SiO$_2$. Based on the above results, Ir-ReO$_x$/SiO$_2$ exhibited remarkable improvement in catalytic activity compared with monometallic and other bimetallic catalysts.

Encouraged by the above promising result, the effect of various supports (Al$_2$O$_3$, MgO, CeO$_2$, ZnO and ZrO$_2$) on the performance was then explored. Figure 1 shows that the catalysts Ir-ReO$_x$/MgO, Ir-ReO$_x$/CeO$_2$, Ir-ReO$_x$/ZnO, and Ir-ReO$_x$/ZrO$_2$ afforded low conversions (< 30%) with the yields of naphthenes less than 20%. While Ir-ReO$_x$/Al$_2$O$_3$ gave much higher conversion up to 92%, but the yield of cyclohexane was only moderate (86%). Exceptionally, unsaturated product ethylbenzene was detected in the yield of 39%. The different catalytic activity for ring saturation may be attributed to the larger surface area of SiO$_2$ compared to Al$_2$O$_3$ (Table S1), which favors the dispersion of Ir species. Nevertheless, Ir-ReO$_x$/SiO$_2$ still showed the highest activity.

Optimization of the reaction conditions (Figures S2-S3) suggested that the proper reaction temperature, hydrogen pressure and time were 260 °C, 2 MPa H$_2$ and 10 h. Figure S2 also showed that the yield of ethyl-cyclohexane increased clearly with the increasing of the reaction temperature and hydrogen

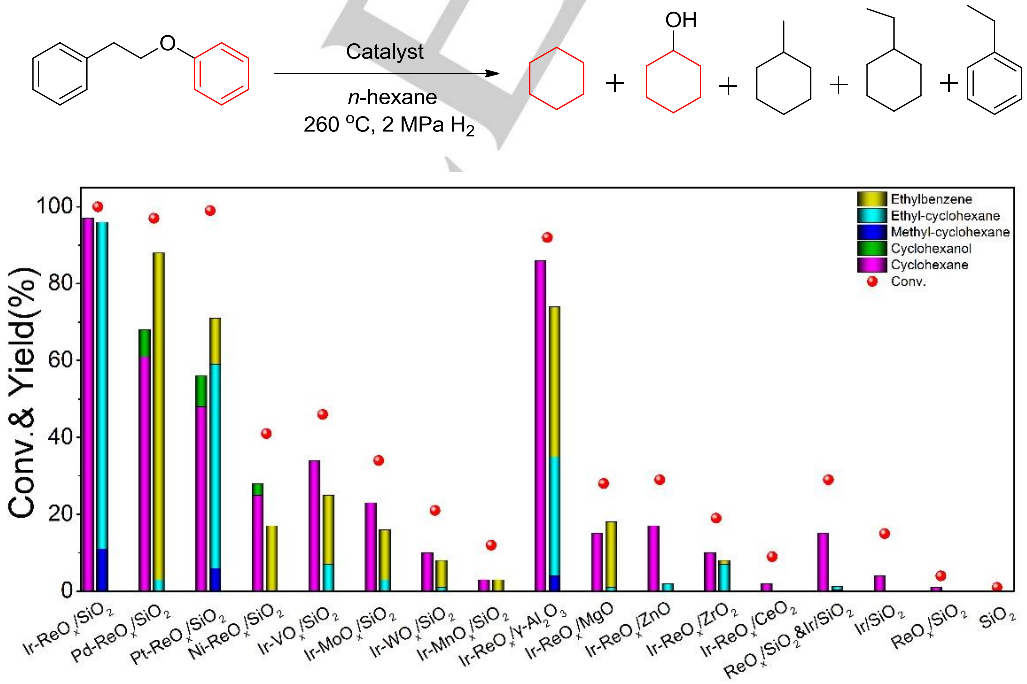

Figure 1. Catalytic performance of various catalysts. The reaction condition: phenethoxybenzene (0.5 mmol), the catalyst (30 mg), n-hexane (30 mL), T = 260 °C, 2MPa H$_2$, t=10 h. Ir/SiO$_2$ (0.2 wt%Ir), ReO$_x$/SiO$_2$(2 wt% Re), Ir-ReO$_x$/SiO$_2$ (0.2 wt% Ir, 2 wt% Re); M-ReO$_x$ /SiO$_2$ (0.2 wt% M, 2 wt% Re, M = Ni, Pt, Pd, Ir); Ir-MO$_x$/SiO$_2$ (0.2 wt% Ir, 2 wt% M, M = Mn, W, Mo, V, Re); Ir-ReO$_x$/MO$_x$ (0.2 wt% Ir, 2 wt% Re, M = Ce, Zr, Zn, Mg, Al, Si).

pressure. By contrast, the yield of ethylbenzene decreased under severe conditions, indicating that for the conversion of phenethoxybenzene, C-O bonds were cleaved first, followed by saturation of aromatic rings to afford cycloalkanes, which is supported by time course profile (Figure S3), which will be further discussed in the following part.

Hydrodeoxygenation of various lignin model compounds

To generalize the protocol, Ir-ReO_x/SiO_2 was employed to convert the mono-phenols that are major components in lignin bio-oil.[6a] As indicated in Table 1, these substrates, belonging to syringyl, guaiacol and coumaryl types of units, reached complete conversion to afford cycloalkanes as the dominant products. From entries 1, 2 and 7, one can find that higher H_2 pressure is required to guarantee the deoxygenation for saturation of the substrates containing more methoxy groups. For instance, phenol was easily converted to cyclohexane quantitatively under 2 MPa H_2 at 260 °C within 10 h (Entry 1). Whereas guaiacol with one methoxy group provided 37% yield of cyclohexane with incomplete hydrogenation product such as 3% yield of cyclohexanol and 9% phenol under the same condition (Entry 2). Higher H_2 pressure of 3 MPa could increase cyclohexane yield to 79%. Similar tendency was observed in the case of 2,6-dimethoxyphenol with two methoxy groups (syringyl subunit), as illustrated by the fact that the yield of cyclohexane improved to 90% yield of cyclohexane under 4 MPa H_2 from 28% yield of cyclohexane and 19% yield of guaiacol under 2 MPa H_2 (entry 7). The above results suggested that the demethoxylation ability is promoted by hydrogen pressure, the activity sequence of the aromatic units follows hydroxyphenyl>guaiacol>syringyl types order under the same condition. Moreover, the substrate with additional C=C bond in sidechain group also needs high H_2 pressure to guarantee the high yield of cycloalkanes (entry 5 vs entry 6). Based on the above results, all monomers have been converted to cycloalkanes under optimized condition, suggesting that Ir-ReO_x/SiO_2 exhibited excellent activity for hydrodeoxygenation of various monomers.

Table 1. Conversion of various lignin monomers into cycloalkanes catalyzed by Ir-ReO_x/SiO_2[a]

Entry	Substrates	C_6 ring Selectivity [%][b]			C_6 ring Balance [%][b]
1[c]	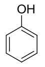 Conv. 100%	 100			100
2	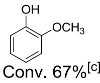 Conv. 67%[c] Conv. 100%	 37[c] 79	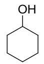 3[c]	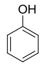 9[c]	49[c] 79
3	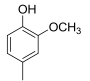 Conv. 100%[c] Conv. 100%	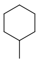 80[c] 93	 3[c] 4	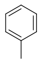 5[c]	88[c] 97
4	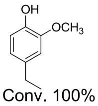 Conv. 100%	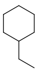 82	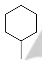 2	 1	85
5	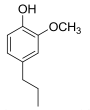 Conv. 100%	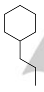 88	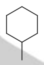 2		90
6	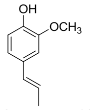 Conv. 100% Conv. 100%[d]	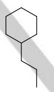 67 80[d]			67 80[d]
7	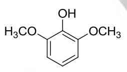 Conv. 95%[c] Conv. 100%[d]	 28[c] 90[d]	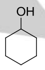 4[c]	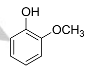 19[c]	51[c] 90[d]

[a]Reaction condition: substrate (0.5 mmol), Ir-ReO_x/SiO_2 (2 wt% Re, 0.2 wt% Ir, 30 mg), T = 260 °C, P = 3 MPa H_2; [b]The C-balance is provided relative to the C_6 ring products owing to demethoxylation; [c] 2 MPa H_2; [d] 4 MPa H_2.

In native lignin, at least two-thirds of the total linkages between the aromatic units are ether bonds such as β-O-4 (β-aryl ether), 4-O-5 (diaryl ether) and α-O-4 (α-aryl ether), and less amount of linkages are C-C bonds (β-β (resinaol), β-5 (phenylcoumaran), 5-5, and β-1 (spirodienone)).[3a] To elucidate the potential application of Ir-ReO_x/SiO_2 in the direct conversion of lignin, model compounds with different types of linkages were tested over Ir-ReO_x/SiO_2. The β-O-4 and α-O-4 model compounds, containing typical ether linkages in lignin, were selectively converted to C_6-C_9 cycloalkanes with the selectivity higher than 55%; meanwhile, C_{13}-C_{14} bicycloalkanes with the selectivity less than 20% were quantified, which were probably generated through randomly free-radical reactions (Entries 1-7).[6a,17] Lercher group also found some secondary recombination products through the ionic and radical mechanism pathways when conversion of α-O-4 model compounds.[18] The comparison experiments of β-O-4 model compounds with different number of OCH_3 groups (Entries 3-7) indicate that more OCH_3 groups would cause lower yield of cycloalkanes under the same condition, and hence high hydrogen pressure is required to guarantee completely removal of OCH_3, which is in agreement with the monomer conversion results (Table 1, entries 2, 3, and 7). It is worth noting that β-O-4 model compound with γ-OH which represents lignin typical realistic segment underwent both C-O bonds cleavage and HDO to give 57% C_6-C_{14} cycloalkanes (Entry 7). Furthermore, 4-O-5 linkage is mainly existence in lignin structure as the unit of oligomer-oligomer couplings and is regarded as the most stubborn ether bonds due to the high bond dissociation energies of aryl-aryl ether bond reaching up to 82.5 kcal/mol.[19] It is interesting to find that in our catalytic systems 4-O-5 model compound diphenyl ether can be efficiently broken down, affording up to 98% selectivity of cyclohexane with quantitative conversion (Entry 8). C-C linkages such as β-1, and 5-5 model compounds, existing in different plant species, were successfully converted to C_{14}, C_{12} and C_6 cycloalkanes, respectively via fully removal of oxygen-containing ketone and hydroxy functional groups (Entries 9-10). On the whole, all these model compounds containing the major linkages of lignin can be effectively converted to naphthenes with different carbon chain without producing any aromatics, indicating that Ir-ReO_x/SiO_2 exhibited superior ability for hydrodeoxygenation and cleavage of C-O bonds. Furthermore, the recycling experiment associated

10.1002/cssc.201903286

Table 2. hydrodeoxygenation of various lignin dimers catalyzed by Ir-ReO$_x$/SiO$_2$[a]

Entry	Substrates	Type	C$_6$ ring Selectivity [%][b]	C$_6$ ring Balance [%][b]
1[c]	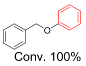 Conv. 100%	α-O-4	 33  31 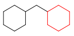 19	83
2	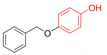 Conv. 100%	α-O-4	 33  32 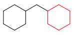 20	85
3	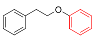 Conv. 100%	β-O-4	 49  6 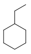 43	98
4	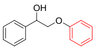 Conv. 100%	β-O-4	 46  4 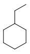 42	92
5	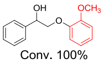 Conv. 100%	β-O-4	 45 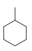 6 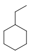 44	95
6[d]	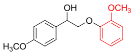 Conv. 100%	β-O-4	 37 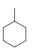 5 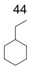 41 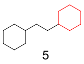 5	88
7[d]	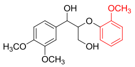 Conv. 100%	β-O-4	 34 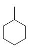 2 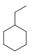 8 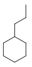 10 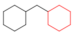 1 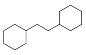 2	57
8	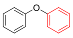 Conv. 100%	4-O-5	 98	98
9	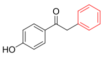 Conv. 100%	β-1	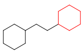 87	87
10	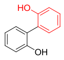 Conv. 100%	5-5	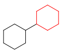 59  4	63

[a]Reaction condition: substrate (0.5 mmol), Ir-ReO$_x$/SiO$_2$ (2 wt% Re, 0.2 wt% Ir, 30 mg), T = 260 °C, P = 3 MPa H$_2$; [b] The C-balance is provided relative to the C6 ring products owing to demethoxylation; [c] 2 MPa H$_2$; [d] 4 MPa H$_2$.

with incomplete conversions for lignin model compounds was carried out (Figure S4). The results showed that Ir-ReO$_x$/SiO$_2$ can be recycled for seven times with a loss in activity, due to the leaching of rhenium oxide species according to ICP-AES characterization (2.02 wt% Re in fresh catalyst vs 1.44 wt% Re in used catalyst; meanwhile, the change of surface composition/property of the catalyst might be another reason for the loss in activity.

With the aim to explore the pathway of different substrates, time course experiments were carried out. According to the results shown in Figure S3, the yields of (2-(cyclohexyloxy)ethyl)benzene and (2-cyclohexylethoxy)benzene were firstly increased, then decreased with prolonging reaction time, indicating that these two dimers are probably the intermediates. The evolutions of ethylbenzene and cylohexanol also indicates that hydrogenation and cleavage of C-O bonds occurred. Thus, it is logical to suppose that the reaction pathway of β-O-4 without hydroxyl group proceed three major pathways (Scheme 1), as aforementioned before. While the substrate with hydroxy and methoxy groups may undergo different routes. Figure S5 shows time-course results using 2-(2-methoxyphenoxy)-1-phenylehtanol as the substrate (Table 2, entry 5). The evolutions of the substrate as well as the products indicate that 2-(2-methoxyphenoxy)-1-phenylehtanol proceeded first hydrodeoxygenation to remove hydroxyl, followed by a cascade C-O bonds cleavage-hydrogenation to obtain cycloalkanes (Scheme 2).

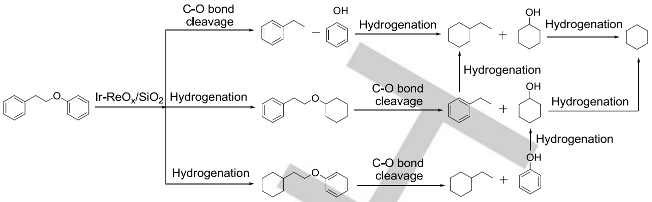

Scheme 1. Proposed reaction pathways of phenethoxybenzene conversion.

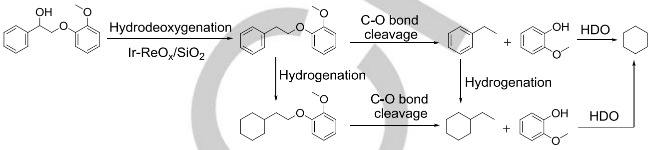

Scheme 2. Proposed reaction pathways of 2-(2-methoxyphenoxy)-1-phenylehtanol conversion.

Characterization of the catalysts

To explore the role of each metal species in Ir-ReO$_x$/SiO$_2$ and unveil the fundamental behind the high catalytic activity, several characterizations of the catalyst were performed. First,

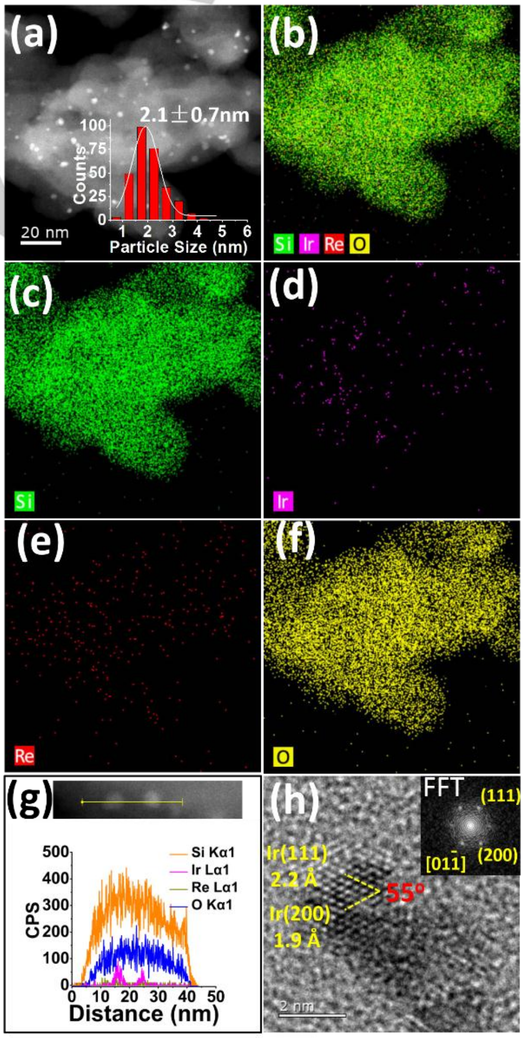

Figure 2. (a) HAADF-STEM images of Ir-ReO$_x$/SiO$_2$, (b, c, d, e, f) STEM-EDX elemental mapping for Si, Ir, Re, O element of Ir-ReO$_x$/SiO$_2$, (g) EDX-linear scanning, (h) the fast Fourier transform (FFT) of Ir-ReO$_x$/SiO$_2$.

10.1002/cssc.201903286

Table 3. Conversion of phenethoxybenzene catalyzed by Ir-ReO$_x$/SiO$_2$.[a]

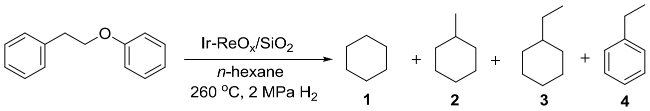

Entry	Catalyst Ir (wt%)-Re(wt%)	Conv. [%][b]	Yield [%][b] 1	 2	 3	 4
1	0.1-2	56	40	1	5	28
2	0.2-2	100	97	11	85	0
3	0.4-2	100	100	15	83	0
4	0.2-5	100	96	15	80	0
5	0.2-1	80	55	2	13	34
6	0.2-0.5	23	10	0	1	7

[a] Reaction condition: substrate (0.5 mmol), Ir-ReO$_x$/SiO$_2$ (30 mg), T = 260 °C, P = 2MPa H$_2$, t = 10 h; [b] The conversion and yields were determined by GC-FID with an internal standard method.

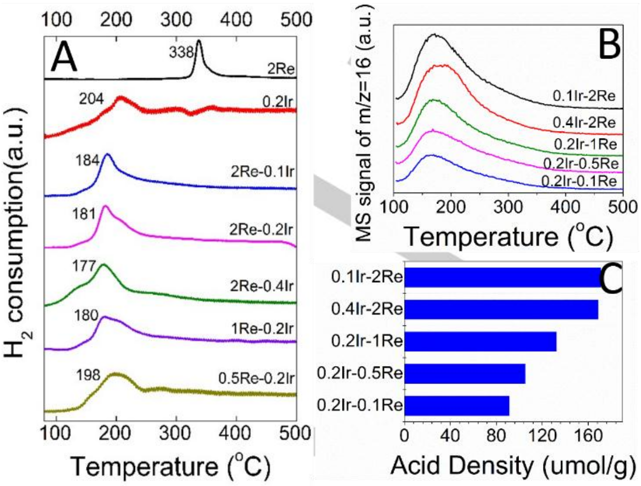

Figure 3. (A) H$_2$-TPR profiles of monometallic and bimetallic catalysts; (B) NH$_3$-TPD profiles and (C) acid content of Ir-ReO$_x$/SiO$_2$.

the XRD profile of Ir-ReO$_x$ /SiO$_2$ (Figure S6) showed no obvious peaks of Re and Ir species, indicating the high dispersion of the metal species on SiO$_2$ support. This fact was also confirmed by the TEM and EDX images in Figure 2. Typical HAADF-STEM images of Ir-ReO$_x$/SiO$_2$ sample together with the corresponding histograms of supported nano-particles (NPs) size distribution (PSD) (Fig. 2a) showed that the NPs are uniformly distributed with mean size of 2.1±0.7 nm. STEM-EDX elemental mapping (Fig. 2b-2f) also demonstrates that Ir and Re are highly dispersed on SiO$_2$. The EDX-linear scanning of single particle (Fig. 2g) exhibits that NPs are IrO$_x$ and ReO$_x$ in the form of even smaller particles, as supported by XPS characterization. The lattice spacings (111) and (200) of Ir with a characteristic acute angle of 55° were identified based on the JCPDS card (No. 46-1044). The results from HRTEM are well consistent with the structure analysis from the fast Fourier transform (FFT) and EDX-linear scanning.

Hydrogen temperature-programmed reduction (H$_2$-TPR) characterization results of various catalysts are presented in Figure 3A, which is used to reveal the redox behavior and the interaction between Ir and ReO$_x$. Monometallic ReO$_x$/SiO$_2$ displayed a sharp hydrogen consumption peak at 338 °C, suggesting that ReO$_x$ alone on the SiO$_2$ support is difficult to be reduced at the reaction temperature of 260 °C, Re species thus is mainly presented as a mixture of high valence of rhenium oxides. The monometallic Ir/SiO$_2$ has a weak signal at 204 °C, hence the in-situ formation of Ir(0) species is likely in charge of hydrogenation in the transformation process at 260 °C. When fixing Re amount in Ir-ReO$_x$/SiO$_2$, H$_2$ consumption peak shifted to lower temperature with increasing of Ir amount, suggesting that the second metal Ir was in favor of decrease the reduction temperature, consequently, it was benefit for hydrogenation reaction. All bimetallic catalysts with different ratio of Ir/Re has lower reduction temperature than both monometallic catalysts (ReO$_x$/SiO$_2$ and Ir/SiO$_2$), providing a direct evidence of synergistic interaction between Ir and Re species, which may have huge effect on catalytic activity. To support the above viewpoint, Ir-ReO$_x$/SiO$_2$ catalysts with different Ir/Re ratios were employed for the conversion of phenethoxybenzene. The results in Table 3 showed that the yield of cyclohexane, methyl-cyclohexane, and ethyl-cyclohenxane increased with an increasing of Ir loading amount when fixing Re content, and unsaturation product ethylbenzene was eventually vanished (entries 1-3). Whilst the yield of ethylbenzene was firstly increased, then decreased in the case of fixing Ir content with increasing Re amount (entries 2, 4-6). Taking H$_2$-TPR characterization (Figure 3A) into consideration, Ir(0) could play an important role for hydrogenation.

The acidic property of Ir-ReO$_x$/SiO$_2$ catalyst was investigated by NH$_3$-TPD and IR spectroscopy of pyridine adsorption. NH$_3$-TPD profiles in Figure 3C revealed that acid amount increases with the increasing of Re content in the bimetallic catalyst. Whilst variation of Ir loading amount has little effect on the acid density according to the results of 0.1Ir-2Re and 0.4Ir-2Re. XPS characterization showed that no Re(0) was formed after reaction, and prolonging the reaction time did not change the composition of Re species (Re^{VI}, Re^{IV}, Re^{II}) greatly (Figure 5), hence Ir-ReO$_x$/SiO$_2$ still possesses the acid sites, despite the acid density decreased after reaction comparing with fresh catalyst (123 vs 169 umol/g) according to NH$_3$-TPD characterization.Therefore, the acidity should be generated from ReO$_x$ species, which would induce acid-catalyzed C-O bond cleavage and facilitate Ir-catalyzed hydrogenolysis reactions.[5a, 20] The acidic property of the catalystwas further confirmed by FTIR spectroscopy of pyridine adsorbed (Figure 4). The IR bands at 1450 cm^{-1} and 1540 cm^{-1} are assigned to Lewis acid and Brønsted acid sites,

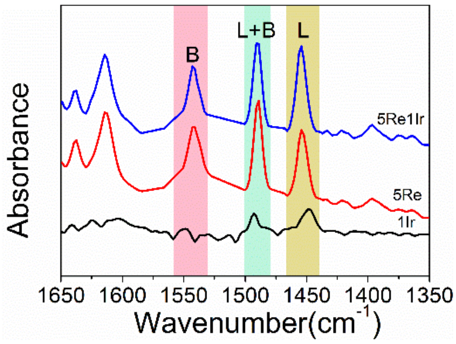

Figure 4. FTIR spectra of adsorbed pyridine on Ir/SiO$_2$, ReO$_x$/SiO$_2$, and Ir-ReO$_x$/SiO$_2$.

10.1002/cssc.201903286

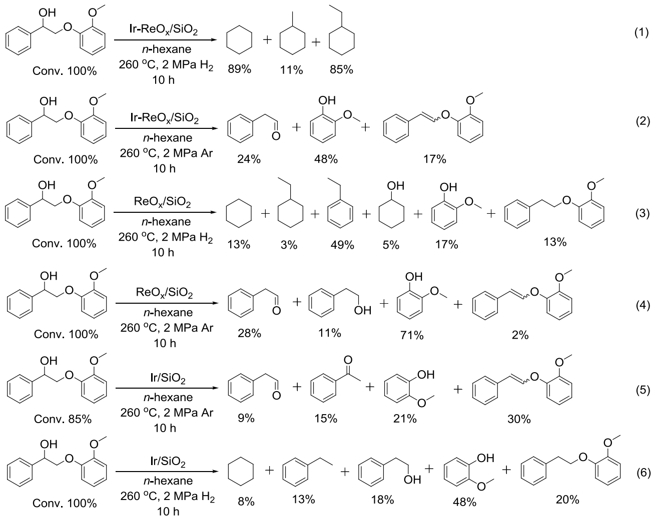

Scheme 3. Control experiments.

respectively; and the band at 1490 cm^{-1} is associated with both Lewis and Brønsted acid sites.[21] Ir/SiO_2 showed a very weak Lewis acid peak at 1440 cm^{-1} whilst Brønsted acid site was absent. In comparison, ReO_x/SiO_2 showed both Lewis and Brønsted acid sites with strong peaks. Interestingly, the IR spectrum of pyridine adsorbed on $Ir-ReO_x/SiO_2$ was similar to that on ReO_x/SiO_2 in peak position, modulating the ration of Lewis and Brønsted acid. In order to investigate the role of each metal in the HDO reaction, several control experiments were carried out. The conversion of 2-(2-methoxyphenoxy)-1-phenylethanol catalyzed by $Ir-ReO_x/SiO_2$ under H_2 afforded complete saturated naphthenes (Equation 1, Scheme 3). In the case of Ar atmosphere, 24% yield of 2-phenylacetaldehyde, 48% yield of guaiacol and 17% yield of 1-methoxy-2-(styryloxy)benzene were obtained, indicating that C-O bondcleavage also occurred. To ascertain the role of rhenium oxides, the same substratecatalyzed by ReO_x/SiO_2 under both H_2 and Ar atmosphere were conducted (Equations 3 and 4). It was found that most of the C-O bonds between the aromatic units were cleaved, suggesting that ReO_x makes major contribution to C-O bond cleavage. The results in Equations 4-5 also gave the same conclusion, because Ir/SiO_2 provided much higher dimer product than ReO_x/SiO_2 under Ar atmosphere (30%vs 2%). It should be noted that in Equation 3, three saturated products were obtained with the yields less than 20% over ReO_x/SiO_2 under H_2, which were much poorer than that obtained in the presence of $Ir-ReO_x/SiO_2$ (Equation 1). These results, in combination with the results of equations 5 and 6 (8% yield of cyclohexane was obtained catalyzed by Ir/SiO_2 in the presence of H_2), indicated that Ir should play a major role in hydrogenation reaction, which is in agreement with H_2-TPR characterization result. Taking into account these comparative conversion results and the above characterizations, it can be concluded that in $Ir-ReO_x/SiO_2$catalyzed 2-(2-methoxyphenoxy)-1-phenylethanol transformation, a synergistic effect between Ir and ReO_x play a crucial role for the high performance, of which, ReO_x was mainly responsible for the cleavage of C-O bond whilst Ir was in charge of HDO reaction and saruration of the benzene rings.

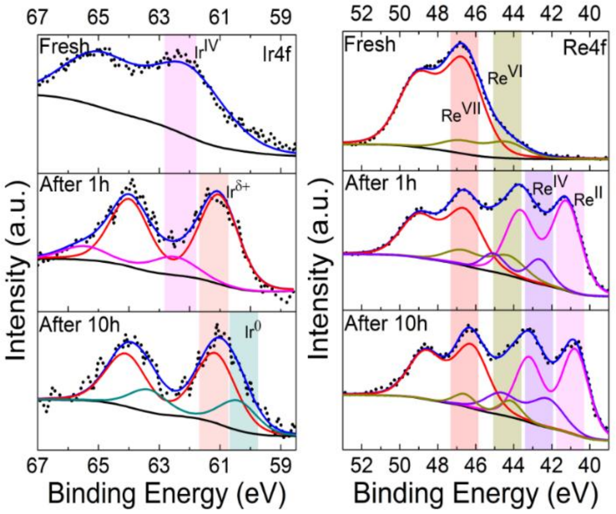

Figure 5. X-ray photoelectron spectra of $Ir-ReO_x/SiO_2$ before and after reaction. (left) Ir 4f, (right) Re 4f.

In order to identify the specific active species, XPS and EXAFS measurements were performed. To avoid oxidation of Re and Ir species, all samples were treated in glove box before XPS and EXAFS measurement. The binding energy (BE) of the surface Re 4f7/2 and Ir 4f2/7 orbitals for $Ir-ReO_x/SiO_2$ are summarized in Figure 5. The Ir4f region gave one contribution on the surface of fresh $Ir-ReO_x/SiO_2$, which was assigned to Ir^{IV}(Ir4f 7/2 = 62.4 eV, IrO_2) specie, which were assigned according to reported value.[22] After 1 h, a new Ir4f7/2 peak at 61.0 eV presented as major proportion, which was assigned to $Ir^{\delta+}$ on the basis of reported reference.[23] Within 10 h, the peak of Ir^{IV} (IrO_2) species was completely disappeared, along with decreasing the amount of $Ir^{\delta+}$. In contrast, Ir^0 specie arose, indicating that Ir^{IV} species was completely reduced to lower valence ones, which was in agreement with H_2-TPR results (Figure 3A). The in-situ generated Ir^0 should be responsible for the hydrogenation

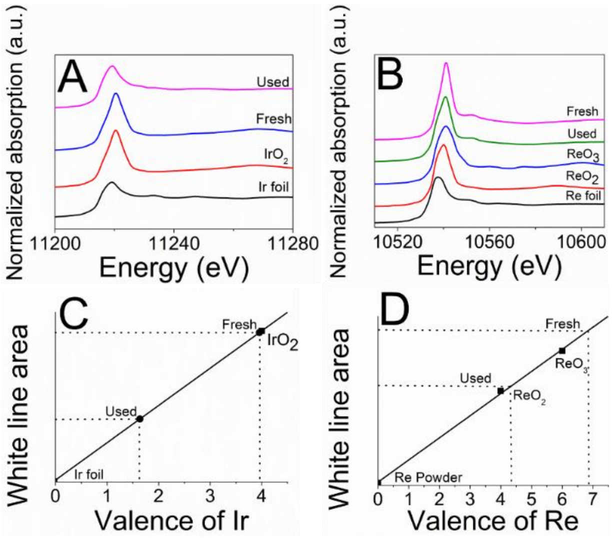

Figure 6. (A, B) The results of Ir L3-edge and Re L3-edge XANES spectra; (C, D) relation between white line area and valence of Ir and Re.

Table 4. Conversion of various lignins into nathphenes over Ir-ReO_x/SiO_2.[a]

Entry	Lignin	Mass/Carbon yield of monomers [%][b][c]				Sum mass/ carbon yield of monomers [%][b][c]	Mass yield of residue [%][d]	Mass/Carbon yield of lignin oil [%][b][c]	Total mass/ carbon yield of naphthenes[%][b][c]
		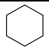	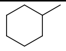	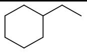	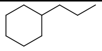				
1	Organosolv lignin	3.2/4.8	6.7/10.1	2.2/3.3	7.2/10.8	19.3/29.0	37.3	11.4/15.3	30.7/44.3
2	Enzymolysis lignin	3.6/5.4	0.7/1.0	3.6/5.4	1.9/2.8	9.8/14.6	30.1	11.6/14.2	21.4/28.8
3	Alkaline lignin	3.1/4.4	0.5/0.7	2.2/3.1	0.8/1.1	6.6/9.3	22.6	14.3/16.6	20.9/25.9

[a]Reaction condition: lignin (300 mg), Ir-ReO_x/SiO_2 (300 mg, 1 wt% Ir, 5 wt% Re), n-hexane = 50 mL, T = 260 °C, P = 4 MPa H_2, t = 10 h; [b] The mass yields were determined by GC-FID with an internal standard method; [c] Carbon yield (%) = ((mass of hydrocarbons × C% in element analysis+mass of monomers × C% in monomers) /mass of original lignin × C% in element analysis) × 100%; Monomers: cyclohexane, methyl-cyclohexane, ethyl-cyclohexane, propyl-cyclohexane; [d] Mass yield of residue (%) = (the weight of the residue/the weight of original lignin) × 100%.

reaction so as to obtain cycloalkanes. In the region of Re4f7/2, fresh Ir-ReO_x/SiO_2 displayed Re^{VII} and Re^{VI} peaks at BEs around 46.5, and 44.2 eV; after reaction 1 h, four peaks at BEs around 46.5, 44.2, 42.4, and 41.0 eV appeared, which were assigned to Re^{VII}, Re^{VI}, Re^{IV}, and Re^{II} respectively, according to reported references.[24] Further prolonging the reaction time did not change the composition of Re species greatly, suggesting that formation of metal Re by H_2 reduction of ReO_x is hard to occur under reaction conditions, which is consistent with H_2-TPR characterization results (Figure 3A). Therefore, Ir^0 could have a major contribution in hydrogenation.

Figure 6 shows the Ir-L3 edge and Re-L3 edge XANES spectra of Ir-ReO_x/SiO_2 before and after reaction. On the basis of white peak area, after reaction the average valences of Ir and Re were decreased from 4.0 to 1.6, and 6.8 to 4.3, respectively. Hence, both XPS and EXAFS characterizations gave the same fact that the metal species in Ir-ReO_x/SiO_2 have been reduced to lower valence states after reaction. Because H_2-TPR characterization has suggested that the metal species in Ir-ReO_x/SiO_2 is easier to be reduced than monometallic catalysts Ir/SiO_2 and ReO_x/SiO_2, the above XPS and EXAFS characterizations further implied that there was an interaction between ReO_x and Ir species, which are in accordance with Tomishige's finding that the interaction between Re and Ir species is presence at above 210 °C reduction temperature.[25] Suchsynergistic effects would increase the metallic property and facilitate the C-O bonds cleavage and HDO process. Based on XPS, EXAFS, H_2-TPR, NH_3-TPD and Pyridine-IR results, Ir^0, which has intrinsic activity in hydrogen-involved reactions, is mainly responsible for hydrogenation/hydrogenolysis reactions, whilst acidic ReO_x facilitates the cleavage of C-O bonds.

Direct conversion of lignin and woody biomass into liquid hydrocarbons

Encouraged by the promising conversion results of lignin monomers and dimers, direct deconstruction of realistic lignins and woody biomass to naphthenes was investigated. Three different sources of lignin, namely, organosolv poplar-lignin, enzymolysis lignin and commercial alkaline-lignin are employed to assess the robustness of the catalytic system. As expected, all three lignins can be deconstructed to naphthenes over Ir-ReO_x/SiO_2 (Table 4 and Figure S7).The carbon yields of the naphthenes were 44.3%, 28.8% and 25.9%, from organosolv lignin, enzymolysis lignin and alkaline lignin, respectively (Table 4), of which, the carbon yield of C7-C9 cyclohexanes (cyclohexane, methyl-cyclohexane, ethyl-cyclohexane, propyl-cyclohexane) were 29.0%, 14.6% and 9.3% respectively. The relative lower yield from alkaline lignin was probably due to higher content of interunit C-C bond in alkaline lignin, which is more difficult to release monomers. Generally, two-step process, i.e. pyrolysis (>350 °C) followed by HDO of the pyrolysis oil involves in the conversion of lignin to napthenes.[6b] In the few cases for the direct conversion of lignin into napthenes (Table S4, entries 1, 3, 4, 6), reaction temperature of 300 °C and hydrogen pressure of 7 MPa are required, to reach so far highest 45% yield of naphthenes.[7] Several researchers also reported upgrading of bio-oil under similar or milder conditions (entries 2 and 5), none of these cases obtained clear better results compared to the current developed catalytic system.

To elucidate the deoxygenation extent of the liquid products and look insight into the structure evolution after reaction, 2D HSQC NMR and GC-MS analysis of the lignin materials and the liquid oils were conducted. GC-MS analysis showed that all compounds were saturated hydrocarbons, and no oxygen containing compound was detected (Figure S7). 2D HSQC NMR characterization further confirms the excellent activity of Ir-ReO_x/SiO_2 in direct dissembling/deoxygenation of lignin. As shown in Figure S8, in aromatic region, three primary aromatic building blocks Syringyl (**S**), guaiacyl (**G**), and *p*-hydroxyphenyl (**H**) units appeared in three fresh lignins. In addition, noncanonical subunits such as p-hydroxybenzoate (**PB**), *p*-coumarate (***p*CA**) and Ferulate (**FA**) moieties were detected in enzymolysis lignin. Interestingly, the signals in aromatic regions almost disappeared for all three corresponding oil products, revealing that the aromatic rings have been saturated after reaction. As a result, the signals in hydrocarbon region of the three liquid oils remarkably increased in comparison with that of the corresponding lignins. Moreover, the signals of β-O-4 (**A**), β-5 (**B**) and β-β (**C**), as well as methoxyl groups in the sidechain region nearly completely vanished for the oil products, illustrating that the major linkages of β-O-4, β-5 and β-β were deconstructed, and methoxyl groups of Syringyl (**S**) and guaiacol (**G**) units were removed. It should be noted that industrial lignin (enzymolysis lignin) and alkaline lignin are well known for their stubborn property that cannot be digested by most of the chemical regents, which are typically a waste stream in paper factory and other biorefinery processes. The conversion of these two lignins revealed that Ir-ReO_x/SiO_2 is an efficient catalyst for converting various lignins to hydrocarbons

(Table S3 and Figure S7). To confirm the activity of the catalyst, the conversion of poplar woody biomass was carried out, giving 3.9% mass yield of oily products (25.2% based on lignin content) and 2.2% mass yield of monomers (14.2% based on lignin content, Table S4 and Figure S9). Additionally, all monomers are the cycloalkanes. Overall, the catalyst has good activity not only in cleavage of the major C-O linkages of lignin, but also for deoxygenation and saturation of both various lignins and raw woody biomass to naphthenes.

Conclusions

We have described a promising catalytic system for the production of naphthenes from lignin over transition metal-modified rhenium oxide catalysts. Ir-ReO_x/SiO_2 exhibited excellent activity on not only lignin model compounds but also realistic lignin feedstocks. The exceptional activity of Ir-ReO_x/SiO_2 is mainly attributed to the synergistic effect between Ir and ReO_x species based on characterization of the catalysts and control experiments. The acid sites generated from ReO_x species facilitates the C-O bonds cleavage, whilst in-situ generated Ir^0 is in charge of hydrogenation in the catalytic process. This facile process could be a promising strategy for the direct conversion of renewable lignin feedstocks into value-added naphthenes.

Experimental Section

Catalyst preparation: all the catalysts were synthesized by wetness impregnation of metal precursors, and then followed by a thermal treatment. First, ReO_x/SiO_2 was synthesized by impregnating the SiO_2 (Qingdao Ocean Chemical Ltd., used after calcination at 700 ºC for 1 h) with an aqueous solution of NH_4ReO_4 (Alfa-Aesar). After drying at room temperature for 12 h and 120 ºC in the oven, ReO_x/SiO_2 was calcined in air at 500 ºC for 3 h. Second, the resulting ReO_x/SiO_2 was impregnated with an aqueous solution of H_2IrCl_6 (Sigma-Aldrich). After drying at room temperature for 12 h, the sample was further dried at 120 ºC in the oven for 12 h, and then was calcined in air at 500 ºC for 3 h with a 10 ºC min^{-1} temperature ramp to obtain Ir-ReO_x/SiO_2 catalyst. The same preparation procedure was followed to synthesize other bimetallic catalysts such as Ir-ReO_x/SM (SM: Al_2O_3 was home-made, and used after calcination at 700 ºC for 1 h; MgO was from Sinopharm Chemical Reagent. Co., Ltd., and used after calcination at 700 ºC for 1 h; CeO_2 was from Sinopharm Chemical Reagent. Co., Ltd. and used after calcination at 600 ºC for 3 h; ZnO and ZrO_2 was from Tianjin Kemiou Chemical Reagent Co. Ltd., used after calcination at 700 ºC for 1 h) and ReO_x-M/SiO_2 (M= Pd, Pt, Ni) as well as MO_x-Ir/SiO_2 (M = V, W, Mo and Mn). The metal precursors were $Pd(NO_3)_2$ (Shanghai 3A Chemical Reagent. Co., Ltd.), $H_2PtCl_6{\cdot}6H_2O$ (Tianjin Fengchuan Chemical Reagent Co., Ltd.), and $Ni(NO_3)_2$ (Tianjin Damao Chemical Reagent Factory), $Mn(NO_3)_2$, NH_4VO_3 as well as $(NH_4)_6H_2W_{12}O_{40}{\cdot}xH_2O$ (Shanghai Aladdin Bio-Chem Technology Co., Ltd.), and $(NH_4)_6Mo_7O_{24}{\cdot}4H_2O$ (Tianjin Kaida Chemical Reagent Co., Ltd.), respectively. The reported metal loadings are on the basis of the theoretical amount of metals used from impregnation. All catalysts were used in the power with granule sized of 40-60 mesh.

Typical procedure for the conversion of lignin model compounds: the parr autoclave (100 mL) was charged with a suspension of 30 mg catalyst, 36 mg n-tridecane as an internal standard, 0.1 g lignin model compounds in 30 mL *n*-hexane. The autoclave was sealed and purged with hydrogen three times to remove air and oxygen, then charged with desired hydrogen pressure at room temperature and stirred (800 rpm). The reaction was heated to the desired reaction temperature. After reaction, the reaction mixture was rapidly cooled to room temperature and filtered. The filtrate was analyzed by GC-MS and quantified with GC-FID by an internal standard method (standard: n-tridecane, HP-5 column, 30 m × 0.32 mm × 0.25 µm). For recycling experiment, after reaction, the solution was filtrated, then the catalyst was dried at 60 ºC within 5 h for next use. In the reaction with a physical mixture of Ir/SiO_2 (0.2 wt% Ir) and ReO_x/SiO_2 (2 wt% Re), the catalysts were sequentially added into the autoclave without premixing of catalysts.

Typical procedure for lignin and woody biomass depolymerization: Organosolv poplar lignin was extracted by a previous method.[26] And enzymolysis lignin was obtained from Shandong Longlive Bio-Technology Co., Ltd, utilizing alkaline extraction method for corn stalk lignin. Commercial alkaline lignin (CAS: 8068-05-1) was obtained in Jianglaishiye Company. The composition of poplar wood is referenced in our previous work.[27] Typically,300 mg of lignin,300 mg of catalyst, and 50 ml of n-hexane were added in the parr autoclave (100 mL). The reaction was performed at 260 ºC with 4 MPa $H_2$and 10 h for conversion of lignin. 1 g of poplar wood, 1 g of catalyst, and 50 ml of n-hexane were added in the parr autoclave (100 mL). The reaction was performed at 260 ºC with 4 MPa $H_2$and 24 h for conversion of poplar wood. After reaction, the reaction mixture was rapidly cooled to room temperature and filtered. The solid residue was washed three times (using 10 ml *n*-hexane each time) and dried in the oven (60 ºC) for 12 h. The filtrate was analyzed by GC-MS, and quantified by GC-FID using an internal standard (standard: *n*-tridecane, HP-5 column, 30 m × 0.32 mm × 0.25 µm). Then the filtrate was concentrated at room temperature overnight to obtain a liquid oil, weight. The monomers (cyclohexane, methyl-cyclohexane, ethyl-cyclohexane, propyl-cyclohexane) were evaporated with solvent in the concentrated process due to their low boiling point, thus were not included in the oily hydrocarbons.

Acknowledgements

Support from the National Natural Science Foundation of China (21878288, 21690080, 21690083), DNL Cooperation Fund CAS (DNL180302), the Strategic Priority Research Program of the Chinese Academy of Sciences (XDB17020100), and National Key R&D Program of China (2016YFA0202801, 2018YFB1501402) is gratefully acknowledged.

Keywords: Lignin • Hydrodeoxygenation • Ir-ReO_x/SiO_2 • Naphthenes

[1] (a) Z. Sun, B. Fridrich, A. de Santi, S. Elangovan, K. Barta, *Chem. Rev.* **2018**, *118*, 614-678; (b) J. Zakzeski, P. C. A. Bruijnincx, A. L. Jongerius, B. M. Weckhuysen, *Chem. Rev.* **2010**, 110, 3552-3559.

[2] F. Cheng, C. E. Brewer, *Renewable Sustainable Energy Rev.***2017**, *72*, 673-722.

[3] (a) C. Li, X. Zhao, A. Wang, G. W. Huber, T. Zhang, *Chem. Rev.* **2015**, *115*, 11559-11624; (b) A. Rahimi, A. Ulbrich, J. J. Coon, S. S. Stahl, *Nature* **2014**, *515*, 249-252.

[4] (a) S. Gillet, M. Aguedo, L. Petitjean, A. R. C. Morais, A. M. da Costa Lopes, R. M. Lukasik, P. T. Anastas, *Green Chem.* **2017**, *19*, 4200-4233; (b) R. Rinaldi, R. Jastrzebski, M. T. Clough, J. Ralph, M. Kennema, P. C. A. Bruijnincx, B. M. Weckhuysen, *Angew. Chem. Int. Ed.* **2016**, *55*, 8164-8215; (c) J. Wen, S. Sun, B. Xue, R. Sun, *Materials*, **2013**, *6*, 359-391.

[5] (a) L. Wang, J. Zhang, X. Yi, A. Zheng, F. Deng, C. Chen, Y. Ji, F. Liu, X. Meng, F.-S. Xiao, *ACS Catal.* **2015**, *5*, 2727-2734; (b) C. Zhao, J. He, A.

A. Lemonidou, X. Li, J. A. Lercher, *J. Catal.* **2011**, *280*, 8-16; (c) C. Zhao, W. Song, J. A. Lercher, *ACS Catal.* **2012**, *2*, 2714-2723; (d) C. Zhao, Y. Kou, A. A. Lemonidou, X. Li, J. A. Lercher, *Angew. Chem. Int. Ed.* **2009**, *48*, 3987-3990; (e) H. Wu, J. Song, C. Xie, C. Wu, C. Chen, B. Han, *ACS Sustainable Chem. Eng.* **2018**, *6*, 2872-2877; (f) W. Zhang, J. Chen, R. Liu, S. Wang, L. Chen, K. Li, *ACS Sustainable Chem. Eng.* **2013**, *2*, 683-691; (g) Y. Nakagawa, M. Ishikawa, M. Tamura, K. Tomishige, *Green Chem.* **2014**, *16*, 2197-2203; (h) N. Yan, C. Zhao, P. J. Dyson, C. Wang, L.-t. Liu, Y. Kou, *ChemSusChem.* **2008**, *1*, 626-629; (i) M. Hua, J. Song, C. Xie, H. Wu, Y. Hu, X. Huang, B. Han,*Green Chem.***2019**, *21*, 5073-5079.

[6] (a) C. Zhao, J. A. Lercher, *Angew. Chem.Int. Ed.* **2012**, *51*, 5935-5940; (b) Z. Cao, M. Dierks, M. T. Clough, I. B. Daltro de Castro, R. Rinaldi, *Joule,* **2018**, *2*, 1118-1133; (c) G. H. Wang, Z. Cao, D. Gu, N. Pfander, A. C. Swertz, B. Spliethoff, H. J. Bongard, C. Weidenthaler, W. Schmidt, R. Rinaldi, F. Schuth, *Angew. Chem. Int. Ed.* **2016**; (d) H. H. Duan, J. C. Dong, X. R. Gu, Y. K. Peng, W. X. Chen, T. Issariyakul, W. K. Myers, M. J. Li, N. Yi, A. F. R. Kilpatrick, Y. Wang, X. S. Zheng, S. F. Ji, Q. Wang, J. T. Feng, D. L. Chen, Y. D. Li, J. C. Buffet, H. C. Liu, S. C. E. Tsang, D. O'Hare, *Nat. Commun.* **2017**, *8*, 591-601.

[7] X. Y. Wang, R. Rinaldi, *Catal. Today* **2016**, *269*, 48-55.

[8] J. Kong, M. He, J. A. Lercher, C. Zhao, *Chem.Commun.* **2015**, *51*, 17580-17583.

[9] (a) Q. Xia, Z. Chen, Y. Shao, X. Gong, H. Wang, X. Liu, S. Parker, X. Han, S. Yang, Y. Wang, *Nature Commun.* **2016**, *7,11162-11172 ;* (b) D. Ma, S. Lu, X. Liu, Y. Guo, Y. Wang,*Chin. J. Catal.* **2019**, *40*, 609-617.

[10] (a) Y. Kuninobu, K. Takai, *Chem. Rev.* **2011**, *111*, 1938-1953; (b) X. Di, G. Lafaye, C. Especel, F. Epron, J. Qi, C. Li, C. Liang, *ChemSusChem.* **2019**, *12*, 807-823; (c) Y. Nakagawa, S. Tazawa, T. Wang, M. Tamura, N. Hiyoshi, K. Okumura, K. Tomishige, *ACS Catal.* **2018**, *8*, 584-595.

[11] (a) M. Shiramizu, F. D. Toste, *Angew. Chem. Int. Ed.* **2013**, *52*, 12905-12909; (b) X. Li, D. Wu, T. Lu, G. Yi, H. Su, Y. Zhang, *Angew. Chem. Int. Ed.* **2014**, *53*, 4200-4204.

[12] L. Sandbrink, E. Klindtworth, H.-U. Islam, A. M. Beale, R. Palkovits, *ACS Catal.* **2016**, *6*, 677-680.

[13] N. Ota, M. Tamura, Y. Nakagawa, K. Okumura, K. Tomishige, *Angew. Chem. Int. Ed.* **2015**, *54*, 1897-1900.

[14] C. Crestini, P. Pro, V. Neri, R. Saladino, *Bioorg. Med. Chem.* **2005**, *13*, 2569-2578.

[15] (a) R. G. Harms, I. I. E. Markovits, M. Drees, W. A. Herrmann, M. Cokoja, F. E. Kühn, *ChemSusChem***2014**, *7*, 429-434; (b) B. J. Hofmann, R. G. Harms, S. P. Schwaminger, R. M. Reich, F. E. Kühn, *J. Catal.* **2019**, *373*, 190-200.

[16] (a) B. Zhang, C. Li, T. Dai, G. W. Huber, A. Wang, T. Zhang, *RSC Adv.* **2015**, *5*, 84967-84973; (b) Z. J. Qi, B. Zhang, J. W. Ji, X. X. Li, T. Dai, H. W. Guo, A. Q. Wang, L. C. Lu, C. Z. Li, *ChemPlusChem* **2018**, *83*, 500-505; (c) B. Zhang, Z. Qi, X. Li, J. Ji, L. Zhang, H. Wang, X. Liu, C. Li,*Green Chem.* **2019**, *21*, 5556-5564; (d) B. Zhang, Z. Qi, X. Li, J. Ji, W. Luo, C. Li, A. Wang, T. Zhang, *ACS Sustainable Chem. Eng.* **2019**, *7*, 208-215.

[17] P. F. Britt, A. C. Buchanan, M. J. Cooney, D. R. Martineau, *J. Org. Chem.* **2000**, *65*, 1376-1389.

[18] (a) V. Roberts, S. Fendt, A. A. Lemonidou, X. B. Li, J. A. Lercher, *Appl. Catal. B-Environ.***2010**, *95*, 71-77; (b) J. Y. He, L. Lu, C. Zhao, D. H. Mei, J. A. Lercher, *J. Catal.* **2014**, *311*, 41-51.

[19] R. Parthasarathi, R. A. Romero, A. Redondo, S. Gnanakaran, *J. Phys. Chem. Lett.* **2011**, *2*, 2660-2666.

[20] D. Hibbitts, Q. Tan, M. Neurock, *J. Catal.* **2014**, *315*, 48-58.

[21] S. Liu, S. Dutta, W. Zheng, N. S. Gould, Z. Cheng, B. Xu, B. Saha, D. G. Vlachos, *ChemSusChem* **2017**, *10*, 3225-3234.

[22] (a) V. Pfeifer, T. E. Jones, J. J. V. Velez, C. Massue, M. T. Greiner, R. Arrigo, D. Teschner, F. Girgsdies, M. Scherzer, J. Allan, M. Hashagen, G. Weinberg, S. Piccinin, M. Havecker, A. Knop-Gericke, R. Schlogl,*Chem. Phys. Phys. Chem.* **2016**, *18*, 2292-2296; (b) C. Massue, V. Pfeifer, M. van Gastel, J. Noack,G. Algara-Siller, S. Cap, R. Schlogl, *ChemSusChem* **2017**, *10*, 4786-4798.

[23] W. X. Cao, L. Lin, H. F. Qi, Q. He, Z. J. Wu, A. Q. Wang, W. H. Luo, T. Zhang, *J. Catal.* **2019**, *373*, 161-172.

[24] J. Okal, W. Tylus, L. Kępiński, *J. Catal.* **2004**, *225*, 498-509.

[25] Y. Amada, H. Watanabe, M. Tamura, Y. Nakagawa, K. Okumura, K. Tomishige, *J. Phys. Chem. C***2012**, *116*, 23503-23514.

[26] H. Guo, B. Zhang, Z. Qi, C. Li, J. Ji, T. Dai, A. Wang, T. Zhang, *ChemSusChem* **2017**, *10*, 523-532.

[27] C. Li, M. Zheng, A. Wang, T. Zhang, *Energy Environ. Sci.* **2012**. *5*, 6383-6390.

10.1002/cssc.201903286

FULL PAPER

Entry for the Table of Contents (Please choose one layout)

FULL PAPER

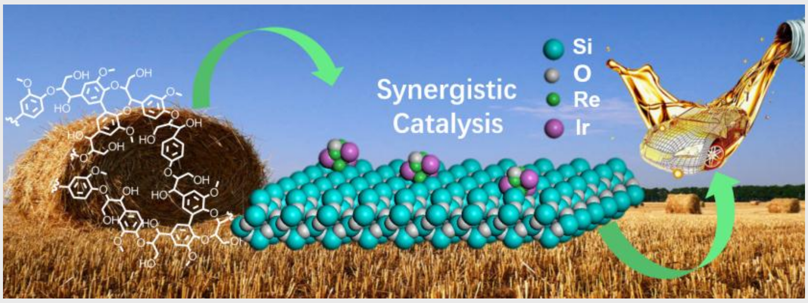

X. Li,[†] *B. Zhang,*[†] *X. Pan, J. Ji, Y. Ren, H. Wang, N. Ji*, Q. Liu, C. Li**

Page No. – Page No.

Heterogeneous Rhenium oxide modified Iridium catalyzed one-port conversion of lignin into naphthenes